Cancer Research

CCL2 Produced by the Glioma Microenvironment Is Essential for the Recruitment of Regulatory T Cells and Myeloid-Derived Suppressor Cells

Alan L. Chang[1,2], Jason Miska[1], Derek A. Wainwright[1], Mahua Dey[3,4], Claudia V. Rivetta[1], Dou Yu[1], Deepak Kanojia[1], Katarzyna C. Pituch[1], Jian Qiao[4,5], Peter Pytel[6], Yu Han[1], Meijing Wu[1], Lingjiao Zhang[4], Craig M. Horbinski[1,7], Atique U. Ahmed[1], and Maciej S. Lesniak[1]

Abstract

In many aggressive cancers, such as glioblastoma multiforme, progression is enabled by local immunosuppression driven by the accumulation of regulatory T cells (Treg) and myeloid-derived suppressor cells (MDSC). However, the mechanistic details of how Tregs and MDSCs are recruited in various tumors are not yet well understood. Here we report that macrophages and microglia within the glioma microenvironment produce CCL2, a chemokine that is critical for recruiting both $CCR4^+$ Treg and $CCR2^+Ly\text{-}6C^+$ monocytic MDSCs in this disease setting. In murine gliomas, we established novel roles for tumor-derived CCL20 and osteoprotegerin in inducing CCL2 production from macrophages and microglia. Tumors grown in CCL2-deficient mice failed to maximally accrue Tregs and monocytic MDSCs. In mixed-bone marrow chimera assays, we found that CCR4-deficient Treg and CCR2-deficient monocytic MDSCs were defective in glioma accumulation. Furthermore, administration of a small-molecule antagonist of CCR4 improved median survival in the model. In clinical specimens of glioblastoma multiforme, elevated levels of CCL2 expression correlated with reduced overall survival of patients. Finally, we found that CD163-positive infiltrating macrophages were a major source of CCL2 in glioblastoma multiforme patients. Collectively, our findings show how glioma cells influence the tumor microenvironment to recruit potent effectors of immunosuppression that drive progression. *Cancer Res; 76(19); 5671–82. ©2016 AACR.*

Introduction

Immune evasion is a major hallmark of tumorigenesis and a potent barrier to effective cancer therapies (1). In a wide spectrum of cancer types, immune evasion manifests as the recruitment of immunosuppressive regulatory T cells (Treg) and myeloid-derived suppressor cells (MDSC) to the tumor microenvironment. Tregs are a FOXP3-expressing subset of $CD4^+$ T cells that play an important role in maintaining immunologic tolerance to self under normal physiologic conditions (2). However, Treg infiltration occurs in a variety of cancer types and is correlated with worse prognosis in breast, ovarian, gastric, and esophageal cancers (3–5). MDSCs are thought to originate from monocytes that gain immunosuppressive capacity under certain pathologic conditions (6, 7). Human MDSCs are characterized by the pan-myeloid marker CD33, with monocytic $CD14^+$ and granulocytic $CD15^+$ subsets. Murine MDSCs are defined as $CD11b^+Gr\text{-}1^+$ cells, with monocytic $Ly\text{-}6C^+$ and granulocytic $Ly\text{-}6G^+$ cellular subsets.

Glioblastoma multiforme (WHO Astrocytoma Grade IV) is the most common malignant adult brain tumor with a dismal prognosis for patients. Median survival of glioblastoma multiforme is just 14.6 months even with the treatment standard of surgery, radiation, and chemotherapy (8). The glioblastoma multiforme microenvironment is characterized by high levels of immunosuppressive cytokines as well as the accumulation of Tregs and MDSCs (9–13). In gliomas, Treg infiltration is higher in glioblastoma multiforme compared with lower grade astrocytomas, though conflicting reports exist on the prognostic value of Treg infiltration (9, 10, 14). Increased peripheral MDSCs have been observed in glioblastoma multiforme patients (15). In addition, monocytes from healthy donors acquire MDSC characteristics when treated with conditioned media from glioblastoma multiforme cell lines (12). Despite the importance of these cells for the progression of glioblastoma multiforme, the mechanistic sequence of events underlying the recruitment of these cells has yet to be elucidated.

CCL2 is a potential candidate chemokine for Treg trafficking to glioma. Supernatant from cultured U251 glioblastoma

[1]Department of Neurological Surgery, Feinberg School of Medicine, Northwestern University, Chicago, Illinois. [2]Committee on Cancer Biology, The University of Chicago, Chicago, Illinois. [3]Department of Neurological Surgery, Indiana University School of Medicine, Indianapolis, Indiana. [4]Section of Neurosurgery, Department of Surgery, The University of Chicago Hospitals, Chicago, Illinois. [5]Department of Pathology, University of Texas Southwestern Medical Center, Dallas, Texas. [6]Department of Pathology, The University of Chicago, Chicago, Illinois. [7]Department of Pathology, Feinberg School of Medicine, Northwestern University, Chicago, Illinois.

Note: Supplementary data for this article are available at Cancer Research Online (http://cancerres.aacrjournals.org/).

Corresponding Author: Maciej S. Lesniak, Northwestern University Feinberg School of Medicine, 676 N St. Clair, Suite 2210, Chicago, IL 60611. Phone: 312-695-6200; Fax; 312-695-4075; E-mail: maciej.lesniak@northwestern.edu

doi: 10.1158/0008-5472.CAN-16-0144

multiforme cells contains soluble CCL2 and can induce Treg migration *in vitro* (16). Patients with glioblastoma multiforme possess an increased percentage of circulating Tregs that express CCR4, a chemokine receptor that binds to CCL2, albeit with lower affinity than for CCL17 and CCL22 (16, 17). CCL2 has also been tied to the migration of MDSCs. CCR2, a high affinity chemokine receptor for CCL2, is found on several different myeloid cell populations, including MDSCs (18). Virally induced gliomas in *Ccl2*$^{-/-}$ mice possess markedly reduced MDSC infiltration (15). Although these studies have implicated a potential role for the CCL2-CCR4/CCR2 axis, the sequence of events from the induction of CCL2 production to the *in vivo* chemokine–chemokine receptor requirements for Tregs and MDSC recruitment remains incompletely understood. We hypothesized that CCL2 recruits both Tregs and MDSCs in glioblastoma multiforme, thus unifying the two immunosuppressive cell subsets under one axis. We sought to determine the clinical relevance of CCL2 in large-scale patient data, identify sources of CCL2, and elucidate the underlying mechanisms driving Treg and MDSC accumulation. In this report, we determined that CCL2 expression is a prognostic factor for patients with glioblastoma multiforme and can be produced by both macrophages as well as glial cells in glioblastoma multiforme patient samples. In addition, we observed that CD163^{+}-infiltrating macrophages contribute to CCL2 production in glioblastoma multiforme patients. In the GL261 immunocompetent murine model of glioblastoma multiforme, we found that tumor-associated macrophages and microglia are major sources of CCL2, which subsequently recruits CCR4-expressing Tregs and CCR2-expressing Ly-6C^{+} monocytic MDSCs. We established novel roles for tumor-derived CCL20 and osteoprotegerin in inducing CCL2 production from macrophages and microglia. Through mixed-bone marrow chimera studies, we observed a role for CCR4 in Treg recruitment and a requirement for CCR2 in the accumulation of monocytic MDSCs in glioma. Finally, using a small-molecule antagonist, we demonstrated that the CCL2–CCR4/2 axis is a relevant therapeutic target in glioblastoma multiforme. Collectively, these studies delineate how microenvironment-derived CCL2 results in the accumulation of Tregs and MDSCs in glioma.

Materials and Methods

Cell culture

GL261 cells (NCI Frederick National Tumor Repository Lab, obtained in 2007) and mixed-cortical cell cultures were cultured in DMEM (Corning) supplemented with 10% FBS, penicillin/streptomycin solution, and Normocin (InvivoGen). Cell line authentication was not conducted at this time. Microglia were cultured in X-VIVO 15 (Lonza). Bone marrow cells, bone marrow-derived macrophages, and Tregs were cultured in RPMI medium 1640 (Corning) supplemented with penicillin/streptomycin, L-glutamine, β-mercaptoethanol, and FBS.

Mice

All mice were bred and housed under SPF conditions in the Carlson Barrier Facility at the University of Chicago (Chicago, IL). Wild-type C57BL/6J mice (Stock 000664), *Ccl2*$^{-/-}$ mice (B6.129S4-*Ccl2*^{tm1Rol}/J, Stock 004434), *Ccr2*$^{RFP/RFP}$ mice [B6.129 (Cg)-*Ccr2*$^{tm2.1Ifc}$/J, Stock 017586], and CD45.1^{+} mice (B6.SJL-*Ptprc*^{a} *Pepc*^{b}/BoyJ, Stock 002014), were purchased from The Jackson Laboratory. *Ccr4*$^{-/-}$ mice were kindly provided by Dr. John Belperio (University of California Los Angeles, Los Angeles, CA).

Patient data

A detailed description can be found in the Supplementary Materials and Methods section.

IHC

A detailed description can be found in the Supplementary Materials and Methods section.

Orthotopic GL261 model of glioblastoma multiforme

A total of 4×10^5 GL261 cells were intracranially (i.c.) implanted as described previously (19). Mice were treated with the small-molecule CCR4 antagonist C 021 dihydrochloride (Tocris) at 15–50 mg/kg doses administered subcutaneously every other day for a total of 5 doses beginning 1 day post-intracranial GL261 implantation.

Immunofluorescence microscopy

A detailed description can be found in the Supplementary Materials and Methods section.

Bone marrow–derived macrophages and cytokine treatment

A detailed description can be found in the Supplementary Materials and Methods section.

Mixed-cortical cell cultures and isolation of microglia

Mixed-cortical cell cultures and isolation of microglia was performed according to a previously published protocol (20).

ELISA

For ELISA, the Ready-Set-Go! Mouse CCL2 ELISA Kit (eBioscience) was used according to manufacturer's protocol.

Antibody array

Supernatant from GL261 cultures or mixed-cortical cell cultures (MCCC) were incubated with the Mouse Cytokine Array C6 (AAM-CYT-6, RayBiotech) and developed according to manufacturer's protocol. Film was scanned and analyzed for densitometry using ImageJ.

Flow cytometry

Tissue preparation and flow cytometric analysis was completed as published previously (19).

Mixed-bone marrow chimera generation and competition assay

Recipient mice at least 6 weeks of age were irradiated with 1100 cGy using a Gammacell 40 Exactor irradiator (Theratronics). twenty-four hours after irradiation, mice were injected with a 1:1 ratio of WT CD45.1^{+} bone marrow cells or bone marrow cells from CCR4-deficient or CCR2-deficient mice. After 6 weeks following bone marrow reconstitution, mice were injected intracranially with GL261 cells and used for experiments.

Statistical analysis

Groups were compared with Student two-tailed *t* test or one-way ANOVA with Tukey test for multiple comparisons as indicated in figure legends. A *P* value of less than 0.05 was considered statistically significant. Survival curves were compared with the log-rank test, corrected using the Bonferroni method if multiple

survival curves were compared. All statistical tests were done using either Prism 6.0 (GraphPad) or Stata (Statacorp).

Study approval

All animal experiments were approved by the Institutional Animal Care and Use Committee at the University of Chicago (Chicago, IL).

Results

CCL2 is a clinically relevant prognostic factor in glioblastoma multiforme patients

To determine the clinical relevance of CCL2, we obtained gene expression data and clinical parameters from glioblastoma multiforme patient data available through The Cancer Genome Atlas

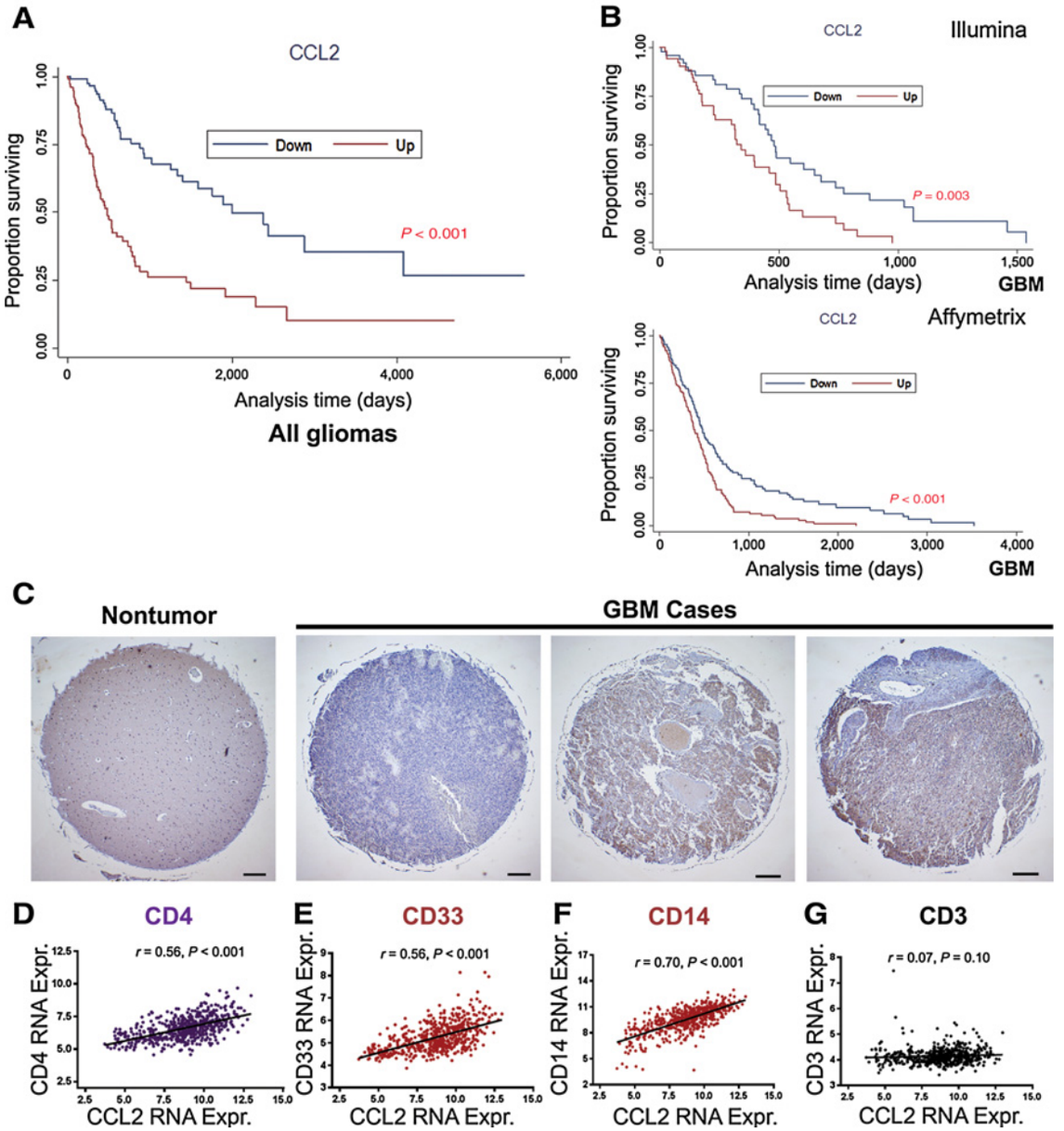

Figure 1.

CCL2 is a clinically relevant chemokine in glioblastoma multiforme on a transcript and protein level. **A,** Kaplan–Meier survival curves of glioma patients (grade I–IV) were generated from TCGA Illumina HiSeq data, where patients were segregated into CCL2-low and CCL2-high expressing groups on the basis of <mean − 0.5SD (for CCL2-down) and >mean + 0.5SD (CCL2-up; CCL2-down, $n = 161$; CCL2-up, $n = 159$). **B,** analysis restricted to glioblastoma multiforme (grade IV) patients for both Illumina HiSeq (CCL2-down, $n = 42$; CCL2-up, $n = 41$; top) and Affymetrix U133A (CCL2-down, $n = 135$; CCL2-up, $n = 134$; bottom) arrays. **C,** representative images from glioblastoma multiforme tissue microarray. Pathology scoring from left to right: 0, 2, 2 on a scale of 0–3. Scale bar, 200 μm. **D–G,** pearson correlation between gene expression from glioblastoma multiforme patient data of CCL2 expression and CD4, CD33, CD14, and CD3. Kaplan–Meier curves were compared using the log-rank test. GBM, glioblastoma mutiforme; RNA Expr., relative mRNA expression.

(TCGA). Patients were stratified into CCL2-high and CCL2-low groups based on CCL2 gene expression. Median survival was significantly increased in CCL2-low subset patients in data encompassing all glioma grades (Fig. 1A) as well as in data limited to glioblastoma multiforme cases alone (Fig. 1B) when compared with the CCL2-high subset (Affymetrix U133A: CCL2-low 479 days, CCL2-high 375 days, $P < 0.001$; Illumina HiSeq: CCL2-low 485 days, CCL2-high 317 days, $P = 0.003$). CCL2 expression was confirmed as a prognostic factor in glioblastoma multiforme patients through both univariate and multivariate Cox regression analysis (HR = 1.11). In contrast to CCL2, gene expression levels of CCL1, CCL3, CCL4, and CCL28 did not segregate glioblastoma multiforme patient survival (Supplementary Fig. S1A–S1D). To survey CCL2 protein levels in glioblastoma multiforme, we performed immunohistochemical staining of CCL2 on a glioblastoma multiforme patient tissue microarray with 35 glioblastoma multiforme cases with 2 cores from each case (Supplementary Fig. S1H and S1I). In non-tumor brain biopsies, CCL2 expression was

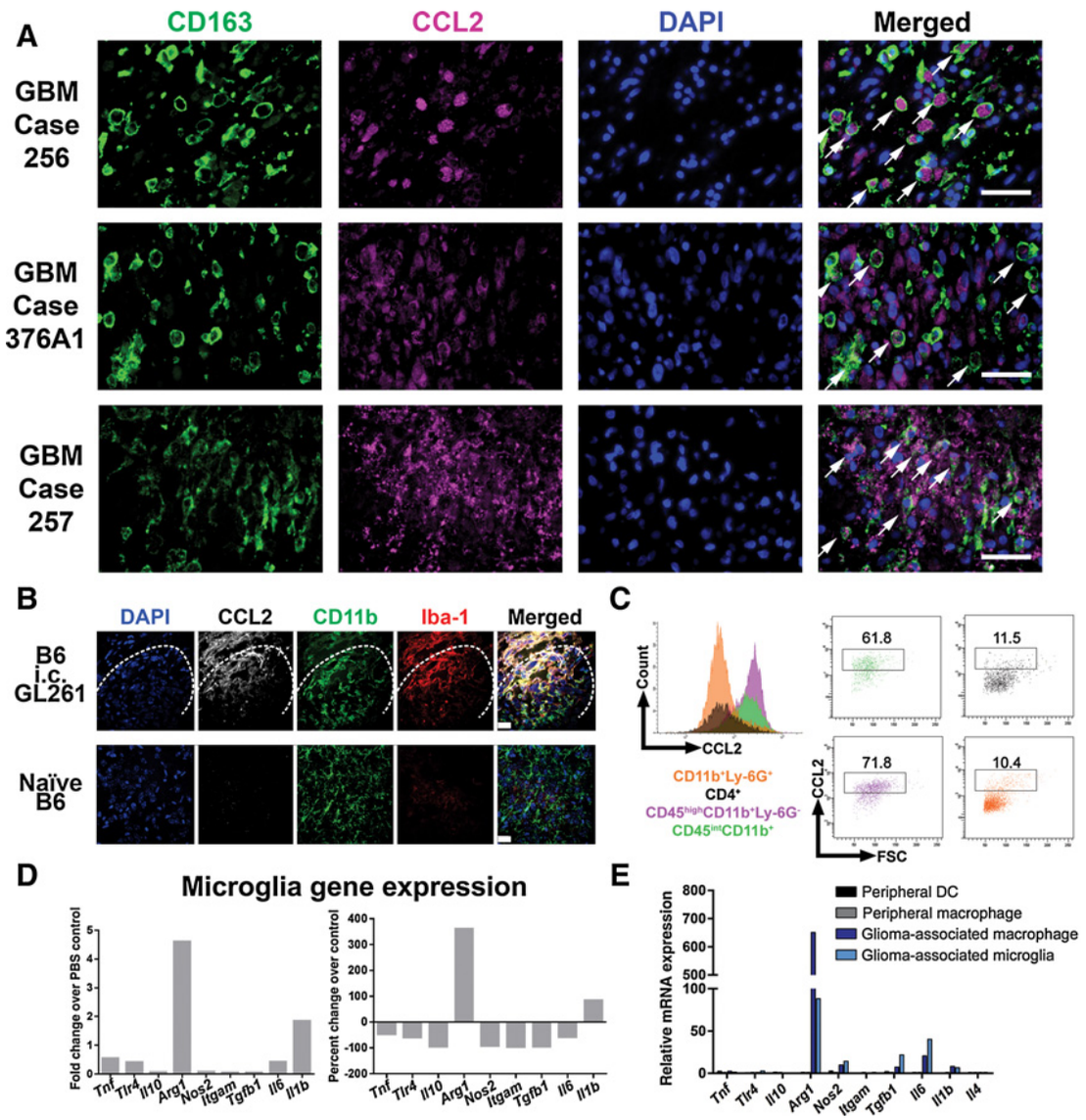

Figure 2.

Myeloid cells are major sources of CCL2 in glioblastoma multiforme patients and GL261 tumors. **A,** double-immunofluorescence labeling of CD163 and CCL2 in glioblastoma multiforme patient tumor samples. Scale bar, 50 μm. Arrows, CCL2-positive, CD163-positive cells. **B,** sections of 1 week post-GL261 implanted or control brains stained for CCL2, CD11b, and Iba1. Dashed line, tumor border. Scale bar, 10 μm. **C,** intracellular cytokine staining of CCL2 in $CD45^{high}CD11b^{+}Ly\text{-}6G^{+}$ macrophages and $CD45^{int}CD11b^{+}$ microglia. **D,** $CD45^{int}CD11b^{+}$ microglia were sorted from tumor-bearing mice ($n = 5$) and gene expression was analyzed by qRT-PCR compared with PBS-injected mice. **E,** expression of M1- and M2-associated genes in glioma-associated microglia and macrophages compared with peripheral macrophages and $CD45^{high}CD11b^{-}CD11c^{+}$ dendritic cells (DC) isolated from spleens within the same mice. Images and plots in (**B** and **C**) are representative of three independent replicates. Data are representative of at least two independent experiments. Data in **A** are represented as mean ± SEM; ****, $P < 0.0001$ by Student's t test.

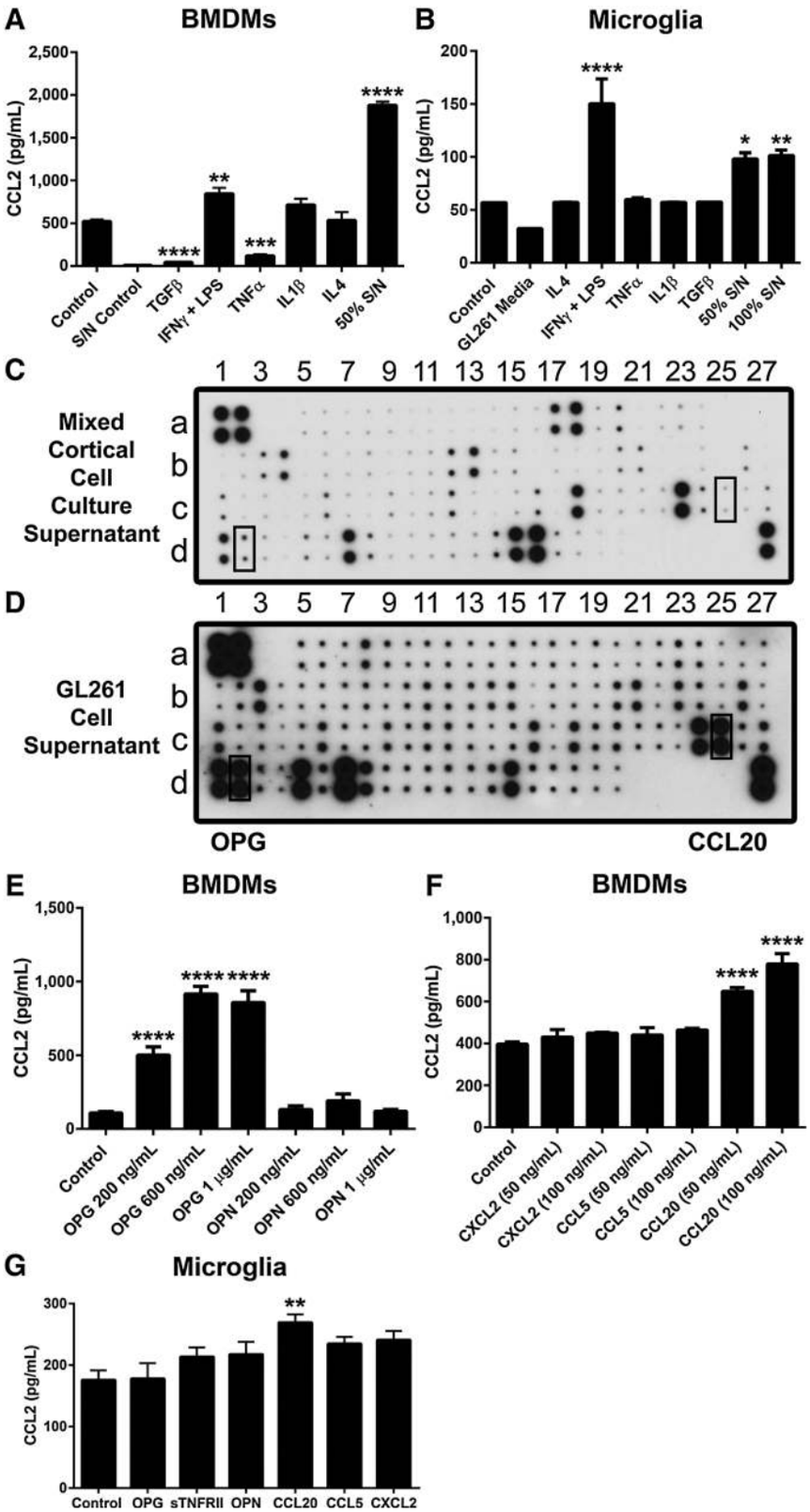

Figure 3.

Soluble tumor-derived factors induce CCL2 secretion by macrophages and microglia. **A,** BMDM were treated for 24 hours with cytokines or media containing 50% GL261 cell supernatant. Supernatant was collected after another 48 hours for CCL2 analysis by ELISA. S/N control denotes the CCL2 content in GL261 supernatant. ($n = 3$–6). **B,** microglia from neonatal MCCC were treated with the indicated cytokines or with media containing GL261 supernatant. ($n = 3$). **C** and **D,** mouse cytokine array from MCCC or GL261 supernatant. **E** and **F,** CCL2 secretion from BMDMs treated with candidate cytokines/chemokines identified from the antibody arrays ($n = 3$–6). **G,** CCL2 secretion from microglia treated with candidate cytokines/chemokines ($n = 3$). Data in **A, B,** and **E–G** are representative of 3–4 independent experiments. Data are represented as mean ± SEM; *, $P < 0.05$; **, $P < 0.01$; ***, $P < 0.001$, and ****, $P < 0.0001$ by ordinary one-way ANOVA with Tukey multiple comparisons test.

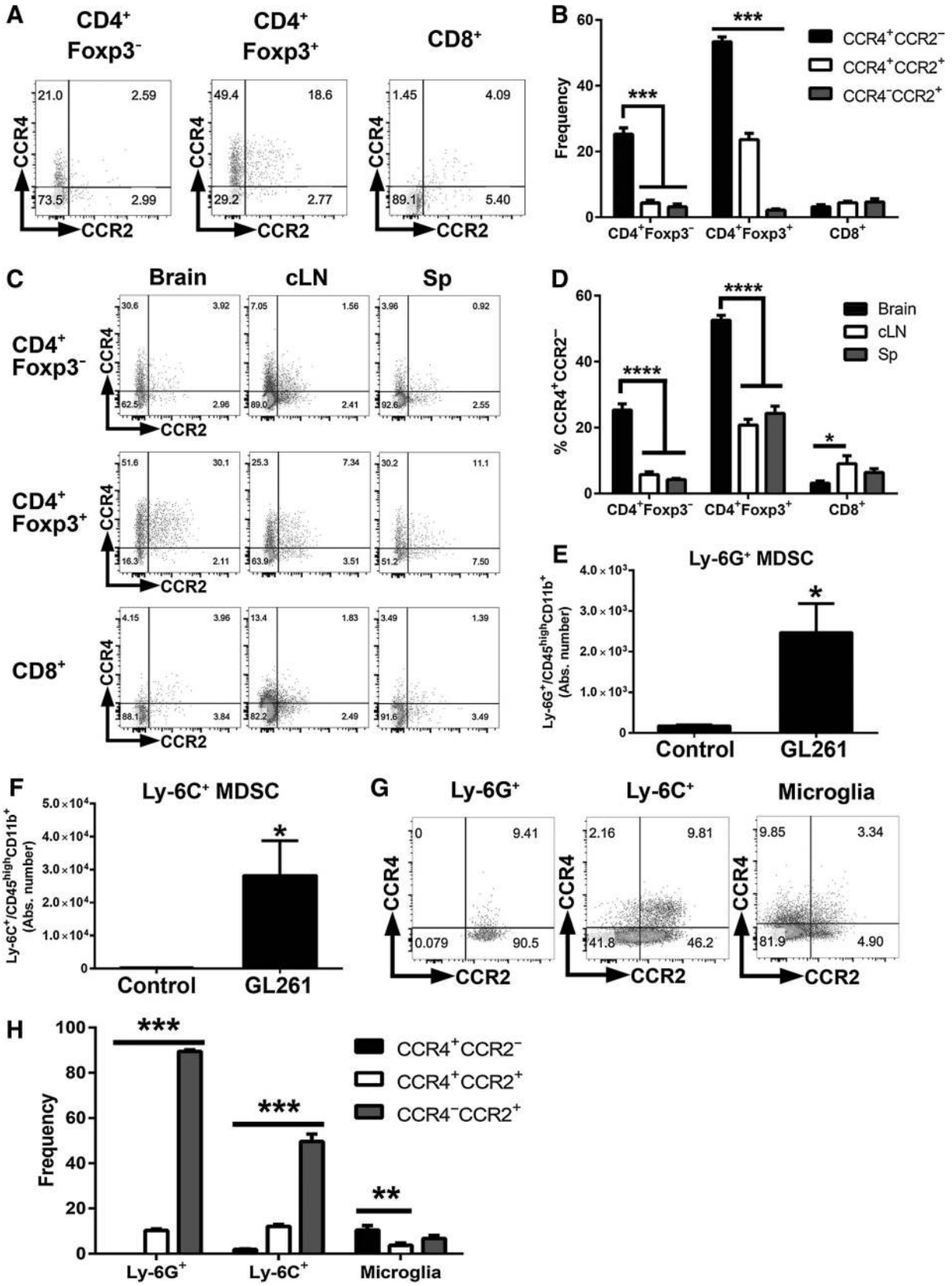

scored as 0 (Fig. 1C, left). In contrast, among the 35 glioblastoma multiforme cases available on the tissue microarray, 16 cases were scored as 0 (no CCL2 staining), 6 cases were scored as 1 (low), 9 cases were scored as 2 (medium), and 4 cases were scored as 3 (highest staining). CCL2 expression was also correlated to the expression of the human MDSC markers CD33 ($r = 0.56$, $P < 0.001$) and CD14 ($r = 0.70$, $P < 0.01$), as well as the expression of CD4 ($r = 0.56$, $P < 0.001$; Fig. 1D–G). Importantly, CCL2 expression was not correlated to the expression of the pan-T-cell marker CD3, implying some specificity to the correlation with CD4 and MDSC markers (Fig. 1G). Overall, the results suggest that CCL2 mRNA expression serves as an important prognostic factor for survival in glioblastoma multiforme and the clinical relevance of CCL2 extends to its presence on a protein level in glioblastoma multiforme patient samples.

CD163-positive macrophages contribute to CCL2 production in glioblastoma multiforme patients

Previous reports have found that CCL2 can be produced by astrocytes in the context of neuroinflammation and by tumor cells in the context of glioma (16, 21, 22). However, because CCL2 can also be produced by tumor-associated macrophages, we sought to determine the respective contributions of glial cells compared with macrophages and microglia for CCL2 production in glioblastoma multiforme patients on a protein level (23, 24). To this end, we performed double-immunofluorescence labeling of CCL2 and the macrophage/microglia marker CD163 in formalin-fixed, paraffin-embedded sections from 20 glioblastoma multiforme patients. We opted for whole sections to ensure extensive anatomic coverage of glioblastoma multiforme tumor areas. We observed heavy infiltration of $CD163^+$ cells that were morphologically infiltrating macrophages in 13 of 20 glioblastoma multiforme cases. CCL2 staining was found in both cellular tumor areas as well as in perinecrotic zones. We observed strong CCL2 immunoreactivity in both $CD163^+$ cells as well as in $CD163^-$ cells in the cases with heavy $CD163^+$ cell infiltration (Fig. 2A). We observed CCL2 immunoreactivity in $CD163^+$ (Fig. 2A, glioblastoma multiforme case 256) as well as in both $CD163^+$ and $CD163^-$ cells (Fig. 2A, glioblastoma multiforme case 376A1 and 257). The $CD163^-$ cells that produce CCL2 are most likely tumor cells, per previous reports. Therefore, both tumor cells as well as glioma-associated macrophages are capable of producing CCL2 in glioblastoma multiforme patients.

CCL2 is a major microenvironment-derived Treg and MDSC-recruiting candidate chemokine in the GL261 model of glioblastoma multiforme

We next investigated the GL261 murine model of glioblastoma multiforme to determine the role of CCL2 directly. In this model, Tregs and MDSCs accumulate in the brain after syngeneic GL261 astrocytoma cells are implanted into C57BL/6 mice (19). We determined CCL2 transcript expression localization in GL261-bearing brains at 1 week after injection, during the recruitment phase for Tregs and MDSCs. Strikingly, high CCL2 transcript levels were found within leukocytes isolated by density gradient centrifugation, approximately 20-fold over PBS control in the whole leukocyte preparation compared with 5-fold over PBS control in nonleukocytes (Supplementary Fig. S2A). CCL2 was also detected on the protein level via ELISA (260 ± 33 ng/mL in the GL261-injected hemisphere compared with 93 ± 7 ng/mL in the non-GL261–injected hemisphere, $P = 0.0075$, mean ± SEM; Supplementary Fig. S2B) and immunofluorescence microscopy (Supplementary Fig. S2C) from the brains of mice at 1 week after intracranial (i.c.) injection of GL261 cells. Furthermore, CCL2 was expressed at the highest level at 1 week post-GL261 injection compared with other candidate Treg and MDSC-recruiting chemokines (Supplementary Fig. S2D). Collectively, these data indicate that CCL2 is present both at the mRNA and protein level in murine brain tumors and that a major source of CCL2 lies within leukocytes in the glioma microenvironment.

$CD11b^+$ macrophages and microglia are the primary source of CCL2 in the GL261 model

To identify the cellular source of CCL2 in the GL261 model, immunofluorescence staining of tissue sections was performed at 1-week after intracranial implantation of GL261 cells (Fig. 2B). CCL2 immunoreactivity was detected in the vicinity of $CD11b^+$ and Iba-1^+ cells only in the context of GL261 brain tumors, but not in the brains of naïve mice. We performed intracellular cytokine staining and found that CCL2 expression was predominantly confined to $CD45^{int}CD11b^+$ microglia (~60% CCL2-positive) and $CD45^{high}CD11b^+$Ly-$6G^-$ macrophages (~70% CCL2-positive; Fig. 2C). In contrast, a low percentage of $CD4^+$ T cells and $CD11b^+$Ly-$6G^+$ granulocytic MDSCs expressed CCL2 (~10% for both $CD4^+$ T cells and granulocytic MDSCs; Fig. 2C). Given that CCL2 can be produced by myeloid cells stimulated with various polarizing conditions, we next determined the M1 or M2 status of glioma-associated microglia and macrophages in our model to identify candidate cytokines responsible for inducing CCL2 production in these cells (25). Microglia from GL261 tumors demonstrated an increased expression of Arginase-1 (*Arg1*) relative to microglia from PBS-injected control brains (Fig. 2D). When compared with peripheral macrophages, glioma-associated macrophages express an approximately 600-fold greater *Arg1* mRNA level while glioma-associated microglia express a 60-fold greater *Arg1* mRNA level (Fig. 2E). Thus, the major sources of CCL2 in GL261 gliomas are *Arg1*-expressing glioma-associated macrophages and microglia.

A soluble GL261-derived factor induces CCL2 production from macrophages and microglia

As tumor-associated macrophages and microglia are major sources of CCL2, we hypothesized that GL261-derived factors induce CCL2 production from these cells. To test this hypothesis,

Figure 4.

GL261 tumors are infiltrated by CCR4-expressing Tregs and CCR2-expressing MDSCs. **A** and **B,** flow cytometric quantification of CCR4 and CCR2 expression among $CD4^+Foxp3^-$ T cells, $CD4^+Foxp3^+$ Tregs, and $CD8^+$ T cells ($n = 5$). **C** and **D,** quantification of CCR4 and CCR2 expression on T-cell subsets in brain compared with cervical lymph nodes and spleen. **E** and **F,** absolute numbers of $CD11b^+$Ly-$6G^+$ and $CD11b^+$Ly-$6C^+$ cells in the brains of tumor-bearing or PBS-injected mice ($n = 5$). **G,** CCR4 and CCR2 expression in MDSC subsets and microglia. **H,** quantification of frequencies in G ($n = 5$). Data are representative of at least four independent experiments. Data are represented as mean ± SEM; *, $P < 0.05$; **, $P < 0.01$; ***, $P < 0.001$, and ****, $P < 0.0001$ by ordinary one-way ANOVA with Tukey multiple comparisons test in **B, D,** and **H** or Student *t* test in **E** and **F**. Sp, spleen.

we treated bone marrow–derived macrophages (BMDM) and microglia isolated from MCCC with conditioned media from GL261 cells. GL261-conditioned media induced CCL2 production from both macrophages (1,881 ± 40 ng/mL in conditioned media–treated macrophages vs. 520 ± 23 ng/mL in control, $P < 0.0001$, mean ± SEM) and microglia (101.3 ± 5.1 ng/mL in conditioned media–treated microglia vs. 56.9 ± 0.1 ng/mL in control, $P < 0.01$) as determined by ELISA (Fig. 3A and B). We also assessed the impact of cytokine stimuli on CCL2 production. LPS + IFNγ induced CCL2 production from BMDMs and microglia, whereas CCL2 production from BMDMs was decreased after treatment with TGFβ or TNFα (42.8 ± 3.9 ng/mL in TGFβ-treated BMDMs and 120.3 ± 15.7 ng/mL in TNFα-treated BMDMs, $P < 0.001$, mean ± SEM; Fig. 3A and B). Collectively, these data suggest that soluble factors derived from GL261 cells induce CCL2 secretion from macrophages and microglia. Consequently, we performed antibody arrays using GL261 supernatant and MCCC supernatant to selectively identify tumor microenvironment-specific soluble factors (Fig. 3C and D; Supplementary Table S1). Using this approach, we identified osteoprotegerin (OPG), osteopontin (OPN), soluble TNF receptor type II (sTNFRII), CCL5, CCL20, and CXCL2. Among these candidate cytokines, only OPG and CCL20 were sufficient to induce CCL2 production *in vitro* (Fig. 3E–G). These data collectively suggest that factors secreted by glioma cells induce CCL2 expression in microglia and macrophages in a non-cell–autonomous fashion.

GL261 tumors are infiltrated by CCR4$^+$ Tregs and CCR2$^+$ MDSCs

We next determined which cells in the glioma microenvironment express chemokine receptors recognizing CCL2. Flow cytometric analysis of GL261-bearing brains at 1 week after tumor implantation found that CCR4 was expressed by 60% CD3$^+$CD4$^+$Foxp3$^+$ Tregs, while CCR2 was localized to CD3$^-$CD45$^+$CD11c$^-$CD11b$^+$ MDSC populations (Fig. 4A and Supplementary Fig. S3). In contrast, CD8$^+$ T cells did not express high percentages of either CCR4 or CCR2 (Fig. 4A and B). The highest percentages of CCR4$^+$ Tregs were observed in the brain compared with cervical lymph nodes (cLN) or the spleen, suggesting that the accumulation of CCR4$^+$ Tregs is specific to brain tumors (Fig. 4C and D). Both MDSC subtypes accumulated in the brain at 1 week after intracranial GL261 implantation and are virtually absent in PBS-injected controls (Fig. 4E and F). Both tumor-infiltrating granulocytic Ly-6G$^+$ MDSCs and monocytic Ly-6C$^+$ MDSCs expressed CCR2 (Fig. 4G and H). In contrast, CD45^{int}CD11b$^+$ microglia expressed minimal CCR2 or CCR4. In total, these results suggest that both Treg and MDSC populations possess chemokine receptors required for responding to CCL2 in the glioma microenvironment.

Tregs and Ly-6C$^+$ monocytic MDSCs fail to maximally accumulate in the glioma microenvironment in the absence of CCL2

To delineate the requirement for CCL2 for the trafficking of Tregs and MDSCs to the tumor microenvironment, we implanted GL261 cells into *Ccl2*$^{-/-}$ mice and analyzed the brain tumor infiltrate at 1 week after implantation. In the absence of CCL2, fewer Tregs (wild-type B6 ~1.52×10^4, *Ccl2*$^{-/-}$ ~6.46×10^3, $P = 0.0260$, mean absolute numbers of CD3$^+$CD4$^+$Foxp3$^+$ Tregs) and monocytic Ly-6C$^+$ MDSCs (wild-type B6 ~7.21×10^4, *Ccl2*$^{-/-}$ ~1.26×10^4, $P = 0.0072$, mean absolute numbers of CD45^{high}CD11c$^-$CD11b$^+$Ly-6C$^+$ monocytic MDSCs) infiltrated the brain tumor in terms of absolute numbers (Fig. 5A and B). Interestingly, the number of infiltrating granulocytic Ly-6G$^+$ MDSCs remained unchanged despite the lack of CCL2 (Fig. 5C). These results indicate that both Tregs and monocytic MDSCs (but not granulocytic MDSCs) require CCL2 for maximal recruitment to gliomas. In addition, these results further support our finding that the glioma microenvironment is the primary source of CCL2, as the GL261 cells implanted into *Ccl2*$^{-/-}$ were CCL2-competent.

Tregs are disproportionately dependent on CCR4 for trafficking to glioma in comparison with effector T cells

Given CCR4 expression on Tregs and CD4$^+$Foxp3$^-$ T cells, we next determined the requirement for CCR4 for brain tumor trafficking. We generated mixed-bone marrow chimeras using bone marrow from wild-type CD45.1$^+$ and CD45.2$^+$*Ccr4*$^{-/-}$ mice, injected the chimeras with GL261 cells, and analyzed the tissues after 1 week (Fig. 5D). A slight deficiency was observed across all T-cell populations within CD45.2$^+$ cells in the brain: Treg (CD45.1$^+$ WT 70.32 vs. CD45.2$^+$*Ccr4*$^{-/-}$ 20.23, $P < 0.0001$, mean frequency), CD4$^+$Foxp3$^-$ (CD45.1$^+$ WT 57.34 vs. CD45.2$^+$*Ccr4*$^{-/-}$ 31.17, $P < 0.001$), and CD8$^+$ (CD45.1$^+$ WT 56.45 vs. CD45.2$^+$*Ccr4*$^{-/-}$ 33.20, $P < 0.0001$; Fig. 5E). However, Treg accumulation in the brain was disproportionately affected by the absence of CCR4, as both CD4$^+$Foxp3$^-$ T-cell/Treg ratios (CD45.1$^+$ WT 0.79 vs. CD45.2$^+$*Ccr4*$^{-/-}$ 1.53, $P = 0.0025$, absolute number ratio) and CD8$^+$ T-cell/Treg ratios (CD45.1$^+$ WT 0.61 vs. CD45.2$^+$*Ccr4*$^{-/-}$ 1.29, $P = 0.0018$, absolute number ratio) were higher in CD45.1$^+$ cells compared with CCR4-deficient CD45.2$^+$ cells (Fig. 5F). CCR4 deficiency had the greatest impact on Treg accumulation in the brain, as the ratio of CD45.1$^+$/CD45.2$^+$ cells was significantly higher among brain tumor-infiltrating Tregs compared with mesenteric lymph nodes (mLN), cLNs, and spleen (Fig. 5G). In contrast, the CD45.1$^+$/CD45.2$^+$ ratio among CD8$^+$ T cells was similar across tissues (Fig. 5G). Monocytic Ly-6C$^+$ MDSCs were not affected by CCR4 deficiency and granulocytic Ly-6G$^+$ MDSC numbers were only marginally affected (Supplementary Fig. S4). Taken together, these results suggest that CCR4 plays a role in the trafficking of T cells to the brain, but is selectively relevant to the recruitment of brain tumor-infiltrating Tregs.

The CCL2-CCR4 chemokine–chemokine receptor interaction is a potential therapeutic target in glioma

We next hypothesized that targeting the CCL2–CCR4 interaction would decrease Treg recruitment in brain tumors. We first assessed the specificity and activity of the small-molecule CCR4 antagonist C 021 *in vitro*. C 021 treatment abrogated Treg chemotaxis to the CCR4 cognate chemokines CCL17 and CCL22 but did not affect Treg migration to RPMI containing 10% FBS and CCL21 (Supplementary Fig. S5A and S5B). To determine the *in vivo* activity of C 021, we treated GL261-implanted mice with 15 mg/kg C 021 administered by subcutaneous injection every other day for five total doses. C 021-treated mice gained a 30% improvement in median survival over vehicle control–treated mice with a commensurate decrease of CCR4$^+$ Tregs and Ly-6G$^+$ MDSCs while infiltrating CD4$^+$ and CD8$^+$ T cells were increased (Supplementary Fig. S6A–S6G). In addition, both CD4:Treg and CD8:Treg ratios were improved in C 021-treated mice (Supplementary Fig. S6H and S6I). Furthermore, dose escalation

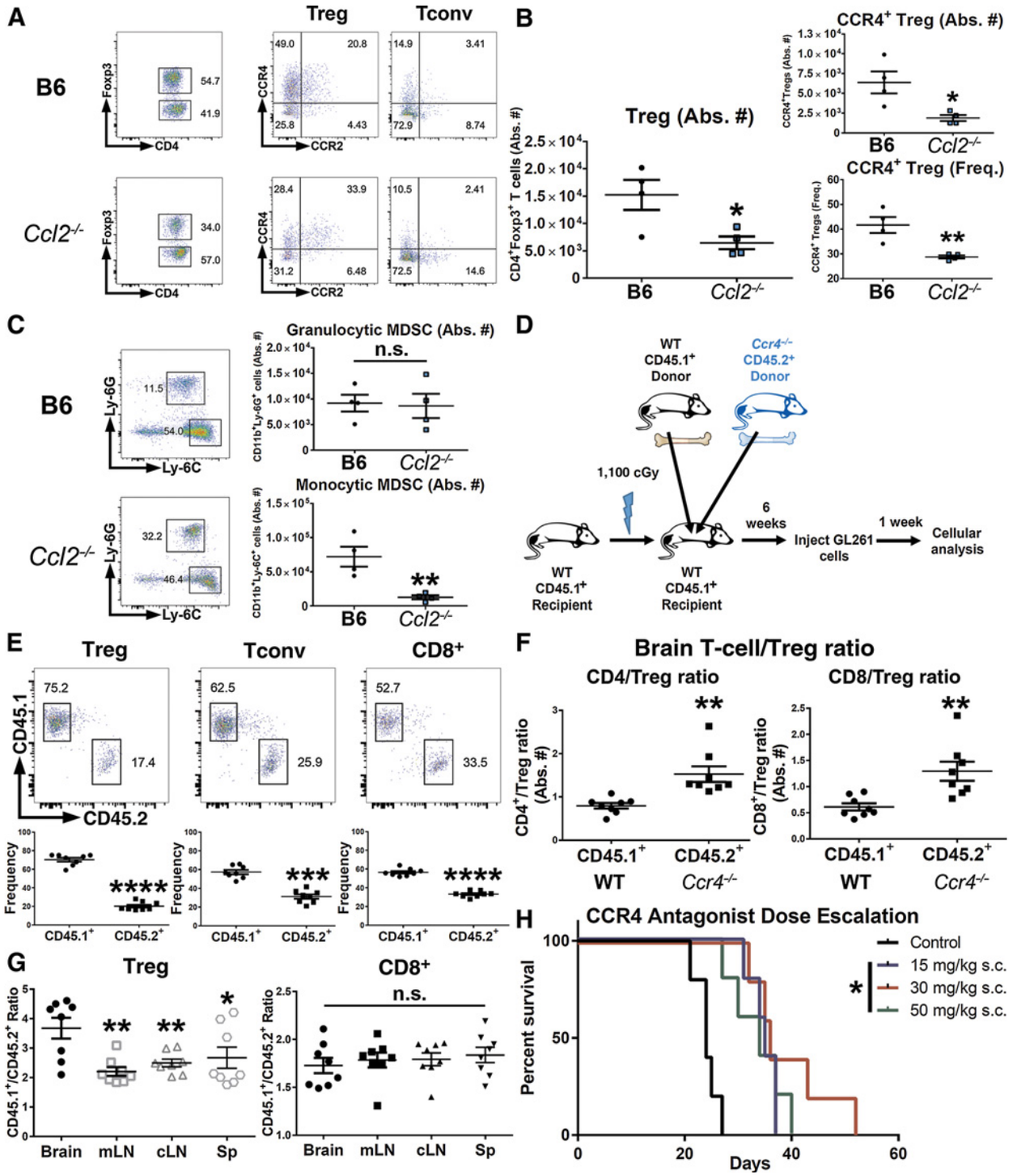

Figure 5.

Mechanistic requirements of CCL2 and CCR4 for trafficking to glioma. **A** and **B,** Treg infiltration at 1 week post-intracranial GL261 in wild-type C57BL/6 (B6) or *Ccl2*$^{-/-}$ mice. ($n = 4$). **C,** MDSCs infiltration in brain tumors of wild-type B6 mice or *Ccl2*$^{-/-}$ mice. **D,** schematic of mixed-bone marrow chimera experiments using wild-type CD45.1$^+$ and CD45.2$^+$*Ccr4*$^{-/-}$ marrow. **E,** flow cytometric analysis of mixed-bone marrow chimera experiments of WT versus *Ccr4*$^{-/-}$ cells within the T-cell compartment. ($n = 8$). **F,** CD4/Treg ratio and CD8/Treg ratio within CCR4-deficient cells or wild-type cells in brain tumor-bearing chimeric mice ($n = 8$). **G,** CD45.1$^+$/CD45.2$^+$ cell ratios in Treg or CD8$^+$ T-cell compartments across tissues in brain tumor-bearing chimeric mice ($n = 8$). **H,** end-point analysis of mice implanted with GL261 cells and treated on alternating days with indicated doses of CCR4 antagonist (C 021) for a total of 5 doses. Data are representative of 2–3 independent experiments. Data are represented as mean ± SEM; *, $P < 0.05$; **, $P < 0.01$; ***, $P < 0.001$, and ****, $P < 0.0001$ by Student *t* test in **B, C, E, F** or ordinary one-way ANOVA with Tukey multiple comparisons test in **G**. Kaplan–Meier survival curves were compared with the log-rank test with the Bonferroni method for multiple comparisons. n.s., nonsignificant.

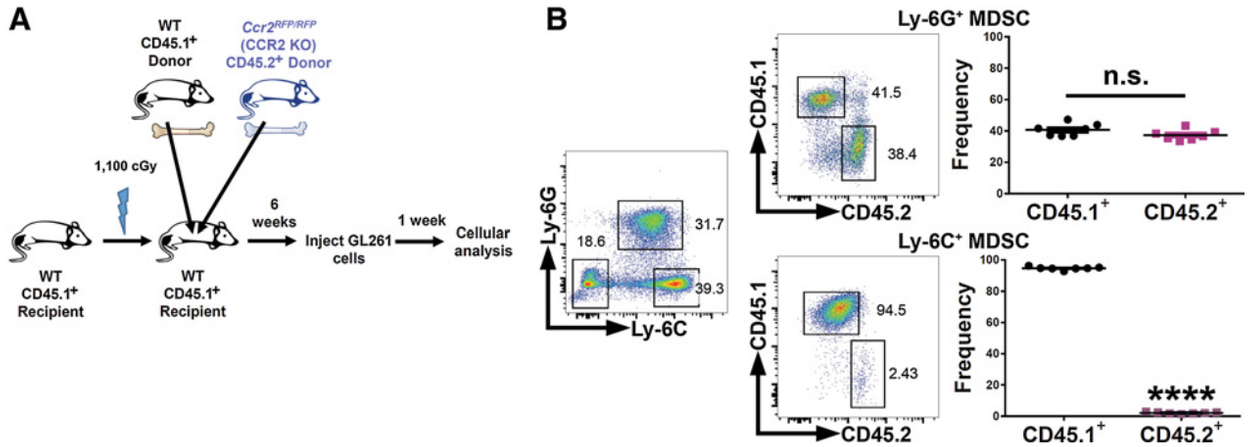

Figure 6.

Ly-6C$^+$ monocytic MDSCs require CCR2 for accumulation in glioma. **A,** schematic of mixed-bone marrow chimera experiments using wild-type CD45.1$^+$ and CD45.2$^+$*Ccr2*$^{RFP/RFP}$ (CCR2-deficient) marrow. **B,** wild-type CD45.1$^+$ or CCR2-deficient CD45.2$^+$ glioma-infiltrating MDSC subsets in brain tumor-bearing chimeric mice ($n = 7$). Data are representative of at least two independent experiments. Data are represented as mean ± SEM; *, $P < 0.05$; **, $P < 0.01$; ***, $P < 0.001$, and ****, $P < 0.0001$ by Student t test. n.s., nonsignificant.

experiments revealed that 15 mg/kg C 021 was sufficient to improve overall survival (Fig. 5H). Thus, the CCR4 chemokine inhibitor selectively inhibits Treg accumulation with the benefit of improved median survival.

Monocytic Ly-6C$^+$ MDSCs that lack CCR2 do not accumulate in glioma

As CCR2 expression was largely localized to MDSCs, we performed a similar mixed-bone marrow chimera competition assay using wild-type CD45.1$^+$ bone marrow and CD45.2$^+$ CCR2-deficient bone marrow (*Ccr2*$^{RFP/RFP}$; Fig. 6A; ref. 26). Within the CD45.2$^+$ CCR2-deficient department, we observed an almost complete lack of Ly-6C$^+$ monocytic MDSCs (Fig. 6B). Ly-6G$^+$ granulocytic MDSCs were unaffected by the absence of CCR2 in terms of trafficking to the brain tumor. Therefore, monocytic Ly-6C$^+$ MDSCs require CCR2 in order for their ultimate accumulation in the GL261 tumors.

Discussion

The immunosuppressive tumor microenvironment remains a major obstacle that impedes productive antitumor immune responses. Here, we have dissected a novel mechanism for Treg and MDSC recruitment that begins with tumor-derived CCL20 and osteoprotegerin inducing CCL2 production from glioma-associated macrophages and microglia (Fig. 7). This mechanistic axis illustrates the potential of macrophages as an additional source of CCL2 in glioblastoma multiforme patients. In the tumor microenvironment, astrocytoma cells are not only capable of producing CCL2 themselves but are also able to induce glioma-associated myeloid cells to secrete CCL2. Importantly, tumor-derived CCL2 and macrophage-derived CCL2 are not necessarily mutually exclusive possibilities. CCL2 then recruits Tregs and MDSCs through CCR4 and CCR2, respectively, as major contributors to the potently immunosuppressive glioma microenvironment.

The protumorigenic or antitumorigenic effects of CCL2 are heavily context-dependent. CCL2-mediated recruitment of MDSCs, monocytes, and macrophages supports colorectal carcinogenesis, endometrial cancer growth, and breast cancer metastasis (27–29). However, anti-CD40 agonist treatment induces CCL2-recruited monocytes degrade fibrosis in an IFNγ-dependent manner, improving gemcitabine efficacy in pancreatic carcinoma (30). CCL2 can also recruit functional antigen-presenting cells in the context of chemotherapy, in which immunogenic cell death is likely to be of major importance (31). Thus, tumors with high amounts of CCL2 may be poised for the induction of a productive immune response if sufficient IFNγ or strongly immunogenic cell death can be induced. In the absence of such initiation, the monocytes and macrophages recruited by CCL2 instead contribute to the immunosuppressive microenvironment together with Tregs trafficking in response to CCL2.

In our mixed-bone marrow chimera studies, we observed some reduction across Treg, CD4$^+$Foxp3$^-$, and CD8$^+$ T-cell populations within the CD45.2$^+$*Ccr4*$^{-/-}$ cells compared with CD45.1$^+$ wild-type cells. Interestingly, this may reflect a minor role for CCR4 in an earlier developmental stage. Aire-dependent expression of CCR4 has been shown to occur during the development of multiple αβ T-cell lineages in the thymus, although CCR4 was not unanimously found to be required for T-cell development in these studies (32, 33). Thus, CCR4 may play a role in the T-cell lineage at the common lymphocyte progenitor stage, during thymic emigration, or even at the level of systemic circulation.

Our observation that MDSC accumulation did not occur in the CCR2-deficient cell compartment parallels other findings that CCR2 deficiency impairs circulating monocyte-dendritic cell progenitors and monocyte progenitors (34). While our analysis does not absolutely decouple the requirement of CCR2 for monocyte trafficking/MDSC trafficking to glioma from that of an earlier monocyte progenitor role, it does confirm a role for CCR2 in the accumulation of glioma-infiltrating monocytic Ly-6C$^+$ MDSCs. Furthermore, differential MDSC subset sensitivity to both CCL2 and CCR2-deficiency is meaningful given that the monocytic MDSC lineage was recently identified as more immunosuppressive in EG7, Lewis lung carcinoma, and B16 tumors (35).

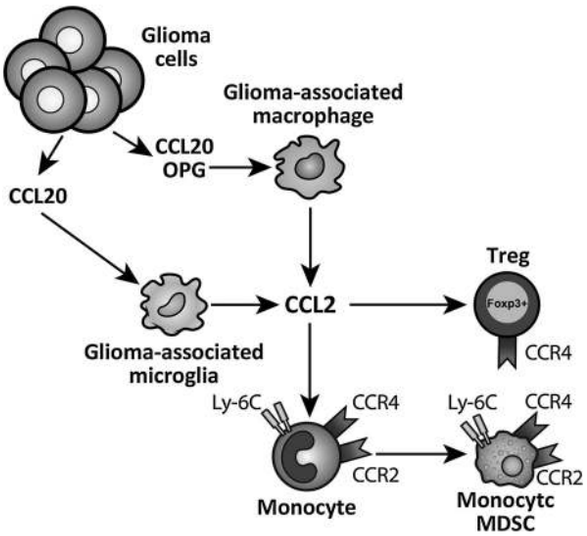

Figure 7.

A model describing the CCL2-CCR4/2 axis in glioblastoma multiforme. Glioma-derived CCL20 and OPG induces the production of CCL2 from glioma-associated macrophages and microglia. CCL2 recruits CCR4-expressing Tregs and CCR2-expressing monocytes to glioblastoma multiforme. These monocytes then differentiate into $CCR2^+$ MDSCs.

Therefore, further characterization of MDSCs in glioblastoma multiforme patients remains an area of considerable interest.

The therapeutic benefit of CCR4 inhibition highlights the potential for other modalities of targeting CCR4, such as with therapeutic antibodies. Mogamulizumab, a defucosylated humanized CCR4 antibody with demonstrated efficacy in T-cell lymphomas, has been adapted for targeting Tregs in solid tumors in a phase Ia clinical trial (36–38). CCR4/2 targeting is likely to be most effective in combination with immunotherapeutic approaches that activate the effector response, such as checkpoint blockade or vaccination to overcome immunosuppression at the tumor site while preventing the additional recruitment of immunosuppressive cells.

CCL2 is likely part of a larger gene expression signature that determines the presence of tumor-infiltrating lymphocyte (TIL)/MDSC/Treg infiltration in glioblastoma multiforme (39–43). As the emphasis on translating immunotherapy for glioblastoma multiforme patients continues to be a priority, identifying factors underlying Treg, MDSC, and TIL recruitment in brain tumors is vital for the strategic disarming of critical immune evasion pathways. Our findings highlight the impact of microenvironment-derived CCL2 in the accumulation of immunosuppressive cells and provide additional critical insight into the barriers that must be overcome for the successful translation of immunotherapies to treat glioblastoma multiforme.

Disclosure of Potential Conflicts of Interest

No potential conflicts of interest were disclosed.

Authors' Contributions

Conception and design: A.L. Chang, J. Miska, D.A. Wainwright, M. Dey, J. Qiao, M.S. Lesniak

Development of methodology: A.L. Chang, J. Miska, M. Dey, C. Horbinski, M.S. Lesniak

Acquisition of data (provided animals, acquired and managed patients, provided facilities, etc.): A.L. Chang, J. Miska, M. Dey, D. Yu, D. Kanojia, K.C. Pituch, P. Pytel, Y. Han, C. Horbinski

Analysis and interpretation of data (e.g., statistical analysis, biostatistics, computational analysis): A.L. Chang, J. Miska, P. Pytel, M. Wu, L. Zhang, C. Horbinski, A.U. Ahmed, M.S. Lesniak

Writing, review, and/or revision of the manuscript: A.L. Chang, J. Miska, D.A. Wainwright, K.C. Pituch, C. Horbinski, A.U. Ahmed, M.S. Lesniak

Administrative, technical, or material support (i.e., reporting or organizing data, constructing databases): C.V. Rivetta, C. Horbinski, M.S. Lesniak

Acknowledgments

The authors thank the Human Tissue Resource Center and the Flow Cytometry Core Facility at the University of Chicago as well as the Northwestern University Nervous System Tumor Bank for technical assistance. We thank Dr. Irina Balyasnikova for helpful comments on the manuscript, Dr. Peter Pytel for pathology scoring, and Dr. Craig Horbinski for pathology scoring and double-immunofluorescence labeling expertise. Finally, the authors thank the TCGA Research Network for glioblastoma multiforme patient data availability.

Grant Support

This work was supported by: NIH NCIR01CA122930 and NINDSR01NS093903 (M.S. Lesniak), NIH NINDSF31NS086365 (A.L. Chang), NIH NCIT32CA009594 (University of Chicago; A.L. Chang)

The costs of publication of this article were defrayed in part by the payment of page charges. This article must therefore be hereby marked *advertisement* in accordance with 18 U.S.C. Section 1734 solely to indicate this fact.

Received January 19, 2016; revised June 11, 2016; accepted July 7, 2016; published OnlineFirst August 16, 2016.

References

1. Hanahan D, Weinberg RA. Hallmarks of cancer: the next generation. Cell 2011;144:646–74.
2. Rudensky AY. Regulatory T cells and Foxp3. Immunol Rev 2011;241:260–8.
3. Curiel TJ, Coukos G, Zou L, Alvarez X, Cheng P, Mottram P, et al. Specific recruitment of regulatory T cells in ovarian carcinoma fosters immune privilege and predicts reduced survival. Nat Med 2004;10:942–9.
4. Bates GJ, Fox SB, Han C, Leek RD, Garcia JF, Harris AL, et al. Quantification of regulatory T cells enables the identification of high-risk breast cancer patients and those at risk of late relapse. J Clin Oncol 2006;24:5373–80.
5. Ichihara F, Kono K, Takahashi A, Kawaida H, Sugai H, Fujii H. Increased populations of regulatory T cells in peripheral blood and tumor-infiltrating lymphocytes in patients with gastric and esophageal cancers. Clin Cancer Res 2003;9:4404–8.
6. Gabrilovich DI, Nagaraj S. Myeloid-derived suppressor cells as regulators of the immune system. Nat Rev Immunol 2009;9:162–74.
7. Khaled YS, Ammori BJ, Elkord E. Myeloid-derived suppressor cells in cancer: recent progress and prospects. Immunol Cell Biol 2013;91:493–502.
8. Stupp R, Mason WP, van den Bent MJ, Weller M, Fisher B, Taphoorn MJ, et al. Radiotherapy plus concomitant and adjuvant temozolomide for glioblastoma. N Engl J Med 2005;352:987–96.
9. Heimberger AB, Abou-Ghazal M, Reina-Ortiz C, Yang DS, Sun W, Qiao W, et al. Incidence and prognostic impact of FoxP3+ regulatory T cells in human gliomas. Clin Cancer Res 2008;14:5166–72.
10. El Andaloussi A, Lesniak MS. CD4+ CD25+ FoxP3+ T-cell infiltration and heme oxygenase-1 expression correlate with tumor grade in human gliomas. J Neurooncol 2007;83:145–52.

11. Crane CA, Ahn BJ, Han SJ, Parsa AT. Soluble factors secreted by glioblastoma cell lines facilitate recruitment, survival, and expansion of regulatory T cells: implications for immunotherapy. Neuro Oncol 2012;14:584–95.
12. Raychaudhuri B, Rayman P, Ireland J, Ko J, Rini B, Borden EC, et al. Myeloid-derived suppressor cell accumulation and function in patients with newly diagnosed glioblastoma. Neuro Oncol 2011;13:591–9.
13. Perng P, Lim M. Immunosuppressive mechanisms of malignant gliomas: parallels at non-CNS sites. Front Oncol 2015;5:153.
14. Fecci PE, Mitchell DA, Whitesides JF, Xie W, Friedman AH, Archer GE, et al. Increased regulatory T-cell fraction amidst a diminished CD4 compartment explains cellular immune defects in patients with malignant glioma. Cancer Res 2006;66:3294–302.
15. Fujita M, Kohanbash G, Fellows-Mayle W, Hamilton RL, Komohara Y, Decker SA, et al. COX-2 blockade suppresses gliomagenesis by inhibiting myeloid-derived suppressor cells. Cancer Res 2011;71:2664–74.
16. Jordan JT, Sun W, Hussain SF, DeAngulo G, Prabhu SS, Heimberger AB. Preferential migration of regulatory T cells mediated by glioma-secreted chemokines can be blocked with chemotherapy. Cancer Immunol Immunother 2008;57:123–31.
17. Zlotnik A, Yoshie O. The chemokine superfamily revisited. Immunity 2012;36:705–16.
18. Lesokhin AM, Hohl TM, Kitano S, Cortez C, Hirschhorn-Cymerman D, Avogadri F, et al. Monocytic CCR2(+) myeloid-derived suppressor cells promote immune escape by limiting activated CD8 T-cell infiltration into the tumor microenvironment. Cancer Res 2012;72:876–86.
19. Wainwright DA, Balyasnikova IV, Chang AL, Ahmed AU, Moon KS, Auffinger B, et al. IDO expression in brain tumors increases the recruitment of regulatory T cells and negatively impacts survival. Clin Cancer Res 2012;18:6110–21.
20. Witting A, Moller T. Microglia cell culture: a primer for the novice. Methods Mol Biol 2011;758:49–66.
21. Ransohoff RM, Hamilton TA, Tani M, Stoler MH, Shick HE, Major JA, et al. Astrocyte expression of mRNA encoding cytokines IP-10 and JE/MCP-1 in experimental autoimmune encephalomyelitis. FASEB J 1993;7:592–600.
22. Carrillo-de Sauvage MA, Gomez A, Ros CM, Ros-Bernal F, Martin ED, Perez-Valles A, et al. CCL2-expressing astrocytes mediate the extravasation of T lymphocytes in the brain. Evidence from patients with glioma and experimental models in vivo. PLoS One 2012;7:e30762.
23. Leung SY, Wong MP, Chung LP, Chan AS, Yuen ST. Monocyte chemoattractant protein-1 expression and macrophage infiltration in gliomas. Acta Neuropathol 1997;93:518–27.
24. Heimdal JH, Olsnes C, Olofsson J, Aarstad HJ. Monocyte and monocyte-derived macrophage secretion of MCP-1 in co-culture with autologous malignant and benign control fragment spheroids. Cancer Immunol Immunother 2001;50:300–6.
25. Cai J, Zhang W, Yang P, Wang Y, Li M, Zhang C, et al. Identification of a 6-cytokine prognostic signature in patients with primary glioblastoma harboring M2 microglia/macrophage phenotype relevance. PLoS One 2015;10:e0126022.
26. Saederup N, Cardona AE, Croft K, Mizutani M, Cotleur AC, Tsou CL, et al. Selective chemokine receptor usage by central nervous system myeloid cells in CCR2-red fluorescent protein knock-in mice. PLoS One 2010;5:e13693.
27. Chun E, Lavoie S, Michaud M, Gallini CA, Kim J, Soucy G, et al. CCL2 promotes colorectal carcinogenesis by enhancing polymorphonuclear myeloid-derived suppressor cell population and function. Cell Rep 2015;12:244–57.
28. Kitamura T, Qian BZ, Soong D, Cassetta L, Noy R, Sugano G, et al. CCL2-induced chemokine cascade promotes breast cancer metastasis by enhancing retention of metastasis-associated macrophages. J Exp Med 2015;212:1043–59.
29. Pena CG, Nakada Y, Saatcioglu HD, Aloisio GM, Cuevas I, Zhang S, et al. LKB1 loss promotes endometrial cancer progression via CCL2-dependent macrophage recruitment. J Clin Invest 2015;125:4063–76.
30. Long KB, Gladney WL, Tooker GM, Graham K, Fraietta JA, Beatty GL. IFNgamma and CCL2 cooperate to redirect tumor-infiltrating monocytes to degrade fibrosis and enhance chemotherapy efficacy in pancreatic carcinoma. Cancer Discov 2016;6:400–13.
31. Ma Y, Mattarollo SR, Adjemian S, Yang H, Aymeric L, Hannani D, et al. CCL2/CCR2-dependent recruitment of functional antigen-presenting cells into tumors upon chemotherapy. Cancer Res 2014;74:436–45.
32. Cowan JE, McCarthy NI, Parnell SM, White AJ, Bacon A, Serge A, et al. Differential requirement for CCR4 and CCR7 during the development of innate and adaptive alphabetaT cells in the adult thymus. J Immunol 2014;193:1204–12.
33. Laan M, Kisand K, Kont V, Moll K, Tserel L, Scott HS, et al. Autoimmune regulator deficiency results in decreased expression of CCR4 and CCR7 ligands and in delayed migration of CD4+ thymocytes. J Immunol 2009;183:7682–91.
34. Yona S, Kim KW, Wolf Y, Mildner A, Varol D, Breker M, et al. Fate mapping reveals origins and dynamics of monocytes and tissue macrophages under homeostasis. Immunity 2013;38:79–91.
35. Haverkamp JM, Smith AM, Weinlich R, Dillon CP, Qualls JE, Neale G, et al. Myeloid-derived suppressor activity is mediated by monocytic lineages maintained by continuous inhibition of extrinsic and intrinsic death pathways. Immunity 2014;41:947–59.
36. Ogura M, Ishida T, Hatake K, Taniwaki M, Ando K, Tobinai K, et al. Multicenter phase II study of mogamulizumab (KW-0761), a defucosylated anti-cc chemokine receptor 4 antibody, in patients with relapsed peripheral T-cell lymphoma and cutaneous T-cell lymphoma. J Clin Oncol 2014;32:1157–63.
37. Duvic M, Pinter-Brown LC, Foss FM, Sokol L, Jorgensen JL, Challagundla P, et al. Phase 1/2 study of mogamulizumab, a defucosylated anti-CCR4 antibody, in previously treated patients with cutaneous T-cell lymphoma. Blood 2015;125:1883–9.
38. Kurose K, Ohue Y, Wada H, Iida S, Ishida T, Kojima T, et al. Phase Ia Study of FoxP3+ CD4 Treg Depletion by Infusion of a Humanized Anti-CCR4 Antibody, KW-0761, in Cancer Patients. Clin Cancer Res 2015;21:4327–36.
39. Thomas AA, Fisher JL, Rahme GJ, Hampton TH, Baron U, Olek S, et al. Regulatory T cells are not a strong predictor of survival for patients with glioblastoma. Neuro Oncol 2015;17:801–9.
40. Sayour EJ, McLendon P, McLendon R, De Leon G, Reynolds R, Kresak J, et al. Increased proportion of FoxP3+ regulatory T cells in tumor infiltrating lymphocytes is associated with tumor recurrence and reduced survival in patients with glioblastoma. Cancer Immunol Immunother 2015;64:419–27.
41. Yue Q, Zhang X, Ye HX, Wang Y, Du ZG, Yao Y, et al. The prognostic value of Foxp3+ tumor-infiltrating lymphocytes in patients with glioblastoma. J Neurooncol 2014;116:251–9.
42. Rutledge WC, Kong J, Gao J, Gutman DA, Cooper LA, Appin C, et al. Tumor-infiltrating lymphocytes in glioblastoma are associated with specific genomic alterations and related to transcriptional class. Clin Cancer Res 2013;19:4951–60.
43. Han S, Zhang C, Li Q, Dong J, Liu Y, Huang Y, et al. Tumour-infiltrating CD4(+) and CD8(+) lymphocytes as predictors of clinical outcome in glioma. Br J Cancer 2014;110:2560–8.